

000
001
002
003
004
005
006
007
008
009
010
011
012
013
014
015
016
017
018
019
020
021
022
023
024
025
026
027
028
029
030
031
032
033
034
035
036
037
038
039
040
041
042
043
044
045
046
047
048
049
050
051
052
053054
055
056
057
058
059
060
061
062
063
064
065
066
067
068
069
070
071
072
073
074
075
076
077
078
079
080
081
082
083
084
085
086
087
088
089
090
091
092
093
094
095
096
097
098
099
100
101
102
103
104
105
106
107

Supplementary materials: Generic Perceptual Loss for Modeling Structured Output Dependencies

Anonymous CVPR 2021 submission

Paper ID 2643

In the supplementary materials, we first give the details of the pilot experiments described in the article. The we show more exploration results about the generic perceptual loss. We first use a toy example to show that random network has the ability to capture the structure information from a global view compared with the pixel-wise L_2 loss. Then we show the impact of the down-sampling operators.

S1. Details of the Pilot Experiment

Most of previous works attribute the success of perceptual loss to the CNN filters pretrained with a large amount of samples. They assume that training for image classification may allow the network to capture high-level features which are coincident to human perception. Although He et al. [9] showed that perceptual loss with the random weight network can work well in solving optimizing problem in the style transfer, it is still interesting to find out if the random weights can work well as a perceptual regularization in training CNNs.

In this pilot experiment, we simply follow the settings in [14], and conduct experiments on a typical image synthesis task, i.e., image super-resolution (SR). We use the popular SRResNet [16] as an SR network. Assume that the input low quality image is I_l , a fully convolutional network can transfer I_l to the estimated high-resolution image \hat{I}_h , and we try to minimize the difference between \hat{I}_h and the real image I_h with per-pixel and perceptual losses following Eq. 1.

$$\ell_{feat}^{\phi,j}(\hat{y}, y) = \frac{1}{C_j H_j W_j} \|\phi_j(\hat{y}) - \phi_j(y)\|_2^2, \quad (1)$$

The per-pixel loss is defined as $\ell_{pixel}(\hat{I}_h, I_h) = \|\hat{I}_h - I_h\|_2^2 / C / H / W$. We assign the perceptual loss network with random weights or pretrained weights for comparison. The super-resolution results are shown in Figure 1 of the main article. We can see that adding the perceptual loss with pretrained and randomized networks can both combat the blurry results in utilizing the per-pixel loss alone.

These observations suggest that the network structure,

instead of the pretrained weights, contributed to the success of the perceptual loss. Through convolution operations in multiple layers, the CNN itself has captured the hierarchical dependencies of variable statistics. By comparing the difference on the perceptual features, a perceptual loss term can be computed to investigate structured dependencies of the inputs. This motivates us to apply the perceptual loss to more structured output learning tasks, in which applying such randomized perceptual loss is non-trivial.

S2. More Explorations

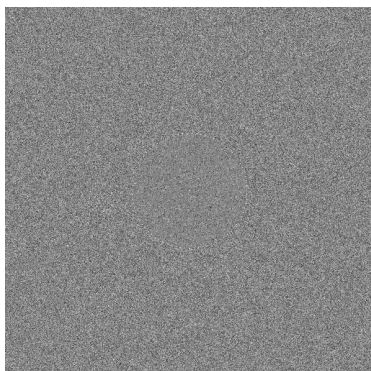
S2.1. Toy Examples

We conduct a toy example to show that the multi layer CNNs have the ability of modeling the structure outputs than a pixel-level L_2 loss. First of all we generate two different backgrounds with the shape of 512×512 using Gaussian noise. The mean is set to 0 and the standard deviation is set to 1. Then, 10000 points with zero values are sampled within the range of a circle with $r = 40$ at the middle of Figure 1a. The exactly same 10000 points are pasted to Figure 1b. Finally, we divided Figure 1a into 16×16 patches, and then random shuffle the patch to generate Figure 1c. Thus, we have a similar pattern of the circle in Figure 1a and Figure 1b.

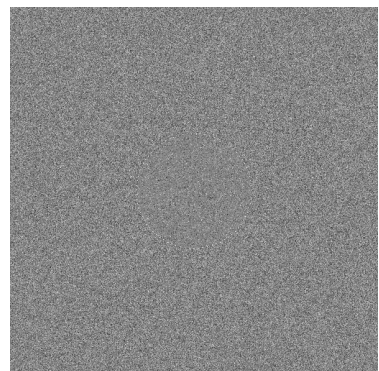
We evaluate the difference between these images under the pixel-level L_2 loss and the genetic perceptual loss initialized with random weights. We run this toy examples for 50 times. In all cases, under evaluation of the pixel-level L_2 loss, Figure 1a and Figure 1c are closer than Figure 1a and Figure 1b, which is contradicted to the perceptual recognition. However, under the evaluation of the perceptual loss, 37 out of 50 trails successfully recognize the similar pattern in Figure 1a and Figure 1b. This indicates that the multi layer CNNs have a stronger ability of modeling the structure outputs than a pixel-level L_2 .

S2.2. Effect of Down-sampling Operators

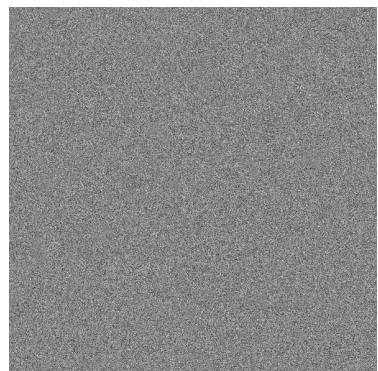
We also explore the ability of down-sampling operators in each block of the perceptual network. Three different

108
109
110
111
112
113
114
115
116
117
118
119
120

(a) Low level noise with a Circle



(b) High level noise with a Circle



(c) Patch Shuffle of (a)

121

122
123
124

Figure 1 – The figure (a) and (b) are generated by the Gaussian noise. We then generated a circle and paste it to the middle of the figure (a) and (b). We finally shuffled the patch of the figure (a), and get (c). Under the evaluation of the pixel-level L_2 , (a) and (c) are closer than (a) and (b), but under the evaluation of the genetic perceptual loss with a random weight network, (a) and (b) are closer.

125

ways are usually employed in the network design: max pooling, average pooling and convolutions with stride of 2. The VGG19 is employed as the basic perceptual network, and we change the down-sampling operators in each block. Following Hamed et al [?], the mapping ability of the random network is evaluated with the classification accuracy on a simple dataset. We fix all the weights except for the final linear classification layer of the random network, and train the final linear layer for 30 epochs on Cifar10. The classification accuracy can reflect the mapping ability of the random network. ‘Mapping’ means to transfer the input into a linearly separable space. In Figure 2, we show the correlation between the segmentation mIoU trained with different perceptual networks, and the mapping abilities. Note that the segmentation network is PSPNet18, and the baseline without perceptual loss can only achieve 69.6% of mIoU. From Figure 2, we can see the classification accuracy on Cifar10 with fixed random network is higher than the chance rate 10%, which means the random network has the ability of mapping the input into a linearly separable space. Besides, with a max pooling layer, the random perceptual loss can achieve the highest performance. Meanwhile, with a max pooling layer, the mapping ability is also higher than other operators. The reason may because with the fix pattern of finding the max value in local region, the saliency of the structure output is easier to be encoded in the embedding space.

153

154
155

References

156
157
158
159
160
161

- [1] Yuanzhouhan Cao, Zifeng Wu, and Chunhua Shen. Estimating depth from monocular images as classification using deep fully convolutional residual networks. *IEEE Trans. Circuits Syst. Video Technol.*, 28(11):3174–3182, 2017.
- [2] Hao Chen, Kunyang Sun, Zhi Tian, Chunhua Shen, Yongming Huang, and Youliang Yan. Blendmask: Top-down

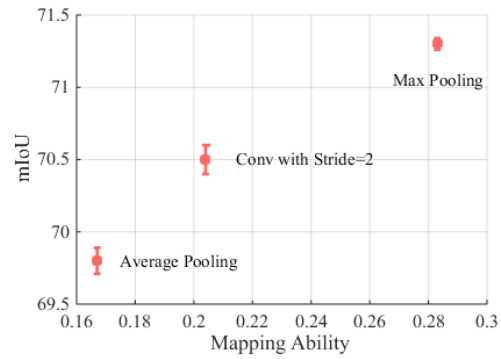
162
163
164
165
166
167
168
169
170
171
172
173
174
175

Figure 2 – Effect of different down-sampling operators. The segmentation network is PSPNet18, and the basic perceptual network is VGG19. Mapping ability means the classification accuracy of the random perceptual network on Cifar10.

meets bottom-up for instance segmentation. In *Proc. IEEE Conf. Comp. Vis. Patt. Recogn.*, pages 8573–8581, 2020.

- [3] Liang-Chieh Chen, Yukun Zhu, George Papandreou, Florian Schroff, and Hartwig Adam. Encoder-decoder with atrous separable convolution for semantic image segmentation. In *Proc. Eur. Conf. Comp. Vis.*, pages 801–818, 2018.
- [4] Marius Cordts, Mohamed Omran, Sebastian Ramos, Timo Rehfeld, Markus Enzweiler, Rodrigo Benenson, Uwe Franke, Stefan Roth, and Bernt Schiele. The cityscapes dataset for semantic urban scene understanding. In *Proc. IEEE Conf. Comp. Vis. Patt. Recogn.*, 2016.
- [5] Mark Everingham, Luc Van Gool, Christopher KI Williams, John Winn, and Andrew Zisserman. The pascal visual object classes (voc) challenge. *Int. J. Comput. Vision*, 88(2):303–338, 2010.
- [6] Huan Fu, Mingming Gong, Chaohui Wang, Kayhan Batmanghelich, and Dacheng Tao. Deep ordinal regression network for monocular depth estimation. In *Proc. IEEE Conf. Comp. Vis. Patt. Recogn.*, pages 2002–2011, 2018.

216 [7] Adam Gaier and David Ha. Weight agnostic neural networks. 270
217 In *Proc. Advances in Neural Inf. Process. Syst.*, pages 5364– 271
218 5378, 2019. 272

219 [8] Leon A. Gatys, Alexander S. Ecker, and Matthias Bethge. 273
220 Image style transfer using convolutional neural networks. In 274
221 *Proc. IEEE Conf. Comp. Vis. Patt. Recogn.*, 2016. 275

222 [9] Kun He, Yan Wang, and John Hopcroft. A powerful 276
223 generative model using random weights for the deep image 277
224 representation. In *Proc. Advances in Neural Inf. Process. Syst.*, 278
225 pages 631–639, 2016. 1 279

226 [10] Kaiming He, Xiangyu Zhang, Shaoqing Ren, and Jian Sun. 280
227 Delving deep into rectifiers: Surpassing human-level 281
228 performance on imagenet classification. In *Proc. IEEE Int. Conf. 282
229 Comp. Vis.*, pages 1026–1034, 2015. 283

230 [11] Kaiming He, Xiangyu Zhang, Shaoqing Ren, and Jian Sun. 284
231 Deep residual learning for image recognition. *Proc. IEEE 285
232 Conf. Comp. Vis. Patt. Recogn.*, pages 770–778, 2016. 286

233 [12] Andrew Ilyas, Shibani Santurkar, Dimitris Tsipras, Logan 287
234 Engstrom, Brandon Tran, and Aleksander Madry. Adversarial 288
235 examples are not bugs, they are features. In *Proc. Advances in 289
236 Neural Inf. Process. Syst.*, pages 125–136, 2019. 290

237 [13] Phillip Isola, Jun-Yan Zhu, Tinghui Zhou, and Alexei Efros. 291
238 Image-to-image translation with conditional adversarial 292
239 networks. In *Proc. IEEE Conf. Comp. Vis. Patt. Recogn.*, pages 293
240 1125–1134, 2017. 294

241 [14] Justin Johnson, Alexandre Alahi, and Li Fei-Fei. Perceptual 295
242 losses for real-time style transfer and super-resolution. In 296
243 *Proc. Eur. Conf. Comp. Vis.*, pages 694–711, 2016. 1 297

244 [15] Alex Krizhevsky, Ilya Sutskever, and Geoffrey Hinton. 298
245 Imagenet classification with deep convolutional neural networks. 299
246 *Comm. of the ACM*, 60(6):84–90, 2017. 300

247 [16] Christian Ledig, Lucas Theis, Ferenc Huszár, Jose Caballero, 301
248 Andrew Cunningham, Alejandro Acosta, Andrew Aitken, 302
249 Alykhan Tejani, Johannes Totz, Zehan Wang, et al. Photorealistic 303
250 single image super-resolution using a generative adversarial 304
251 network. In *Proc. IEEE Conf. Comp. Vis. Patt. Recogn.*, pages 305
252 4681–4690, 2017. 306

253 [17] Guosheng Lin, Chunhua Shen, Anton van den Hengel, and 307
254 Ian Reid. Efficient piecewise training of deep structured 308
255 models for semantic segmentation. In *Proc. IEEE Conf. Comp. 309
256 Comp. Vis. Patt. Recogn.*, pages 3194–3203, 2016. 310

257 [18] Yifan Liu, Ke Chen, Chris Liu, Zengchang Qin, Zhenbo Luo, 311
258 and Jingdong Wang. Structured knowledge distillation for 312
259 semantic segmentation. In *Proc. IEEE Conf. Comp. Vis. Patt. 313
260 Recogn.*, pages 2604–2613, 2019. 314

261 [19] Mihir Mongia, Kundan Kumar, Akram Erraqabi, and Yoshua 315
262 Bengio. On random weights for texture generation in one 316
263 layer CNNs. In *Proc. IEEE Int. Conf. Acous., Speech & 317
264 Signal Process.*, pages 2207–2211, 2017. 318

265 [20] Reiichiro Nakano. A discussion of ‘adversarial examples 319
266 are not bugs, they are features’: Adversarially robust neural 320
267 style transfer. *Distill*, 4(8), 2019. 321

268 [21] Pushmeet Kohli, Nathan Silberman, Derek Hoiem, and Rob 322
269 Fergus. Indoor segmentation and support inference from 323
270 RGBD images. In *Proc. Eur. Conf. Comp. Vis.*, 2012. 324

271 [22] Mark Sandler, Andrew Howard, Menglong Zhu, Andrey Zho- 325
272 moginov, and Liang-Chieh Chen. Mobilenetv2: Inverted 326
273 residuals and linear bottlenecks. In *Proc. IEEE Conf. Comp. 327
274 Vis. Patt. Recogn.*, 2018. 328

275 [23] Karen Simonyan and Andrew Zisserman. Very deep 329
276 convolutional networks for large-scale image recognition. *Proc. 330
277 Int. Conf. Learn. Representations*, 2015. 331

278 [24] Dong Su, Huan Zhang, Hongge Chen, Jinfeng Yi, Pin-Yu 332
279 Chen, and Yupeng Gao. Is robustness the cost of accuracy?— 333
280 a comprehensive study on the robustness of 18 deep image 334
281 classification models. In *Proc. Eur. Conf. Comp. Vis.*, pages 335
282 631–648, 2018. 336

283 [25] Christian Szegedy, Wei Liu, Yangqing Jia, Pierre Sermanet, 337
284 Scott Reed, Dragomir Anguelov, Dumitru Erhan, Vincent 338
285 Vanhoucke, and Andrew Rabinovich. Going deeper with 339
286 convolutions. In *Proc. IEEE Conf. Comp. Vis. Patt. Recogn.*, 340
287 pages 1–9, 2015. 341

288 [26] Zhi Tian, Chunhua Shen, and Hao Chen. Conditional 342
289 convolutions for instance segmentation. In *Proc. Eur. Conf. Comp. 343
290 Vis.*, 2020. 344

291 [27] Zhi Tian, Chunhua Shen, Hao Chen, and Tong He. FCOS: 345
292 Fully convolutional one-stage object detection. In *Proc. 346
293 IEEE Int. Conf. Comp. Vis.*, pages 9627–9636, 2019. 347

294 [28] Dmitry Ulyanov, Andrea Vedaldi, and Victor Lempitsky. 348
295 Deep image prior. In *Proc. IEEE Conf. Comp. Vis. Patt. 349
296 Recogn.*, 2018. 350

297 [29] Hu Wang, Guansong Pang, Chunhua Shen, and Congbo Ma. 351
298 Unsupervised representation learning by predicting random 352
299 distances. *Proc. Int. Joint Conf. Artificial Intell.*, 2019. 353

300 [30] Jingdong Wang, Ke Sun, Tianheng Cheng, Borui Jiang, 354
301 Chaorui Deng, Yang Zhao, Dong Liu, Yadong Mu, Mingkui 355
302 Tan, Xinggang Wang, et al. Deep high-resolution 356
303 representation learning for visual recognition. *IEEE Trans. Pattern 357
304 Anal. Mach. Intell.*, 2020. 358

305 [31] Lijun Wang, Jianming Zhang, Yifan Wang, Huchuan Lu, and 359
306 Xiang Ruan. Cliffnet for monocular depth estimation with 360
307 hierarchical embedding loss. In *Proc. Eur. Conf. Comp. Vis.*, 361
308 pages 316–331, 2020. 362

309 [32] Ting-Chun Wang, Ming-Yu Liu, Jun-Yan Zhu, Andrew Tao, 363
310 Jan Kautz, and Bryan Catanzaro. High-resolution image 364
311 synthesis and semantic manipulation with conditional gans. In 365
312 *Proc. IEEE Conf. Comp. Vis. Patt. Recogn.*, pages 8798– 366
313 8807, 2018. 367

314 [33] Xinlong Wang, Wei Yin, Tao Kong, Yuning Jiang, Lei Li, 368
315 and Chunhua Shen. Task-aware monocular depth estimation 369
316 for 3d object detection. In *Proc. AAAI Conf. Artificial Intell.*, 370
317 volume 34, pages 12257–12264, 2020. 371

318 [34] Xinlong Wang, Rufeng Zhang, Tao Kong, Lei Li, and Chun- 372
319hua Shen. Solov2: Dynamic, faster and stronger. *Proc. Adv- 373
320ances in Neural Inf. Process. Syst.*, 2020. 374

321 [35] Yin Wei, Yifan Liu, Chunhua Shen, and Youliang Yan. En- 375
322 forcing geometric constraints of virtual normal for depth 376
323 prediction. *Proc. IEEE Int. Conf. Comp. Vis.*, 2019. 377

324 [36] Wei Yin, Jianming Zhang, Oliver Wang, Simon Niklaus, 378
325 Long Mai, Simon Chen, and Chunhua Shen. Learning to 379
326 recover 3d scene shape from a single image. In *Proc. IEEE 380
327 Conf. Comp. Vis. Patt. Recogn.*, 2021. 381

328 [37] Changqian Yu, Yifan Liu, Changxin Gao, Chunhua Shen, 382
329 and Nong Sang. Representative graph neural network. *Proc. 383
330 Eur. Conf. Comp. Vis.*, 2020. 384

324	[38] Hengshuang Zhao, Jianping Shi, Xiaojuan Qi, Xiaogang	378
325	Wang, and Jiaya Jia. Pyramid scene parsing network. In	379
326	<i>Proc. IEEE Conf. Comp. Vis. Patt. Recogn.</i> , pages 2881–	380
327	2890, 2017.	381
328	[39] Bolei Zhou, Hang Zhao, Xavier Puig, Sanja Fidler, Adela	382
329	Barriuso, and Antonio Torralba. Scene parsing through	383
330	ade20k dataset. In <i>Proc. IEEE Conf. Comp. Vis. Patt.</i>	384
331	<i>Recogn.</i> , 2017.	385
332		386
333		387
334		388
335		389
336		390
337		391
338		392
339		393
340		394
341		395
342		396
343		397
344		398
345		399
346		400
347		401
348		402
349		403
350		404
351		405
352		406
353		407
354		408
355		409
356		410
357		411
358		412
359		413
360		414
361		415
362		416
363		417
364		418
365		419
366		420
367		421
368		422
369		423
370		424
371		425
372		426
373		427
374		428
375		429
376		430
377		431